Sobolev Regularity Estimation for *hp*–Adaptive Finite Element Methods

Paul Houston[1,*], Bill Senior[1,*], and Endre Süli[2]

[1] Department of Mathematics & Computer Science, University of Leicester, Leicester LE1 7RH, UK
[2] University of Oxford, Computing Laboratory, Wolfson Building, Parks Road, Oxford OX1 3QD, UK

Abstract. In this paper we develop an algorithm for estimating the local Sobolev regularity index of a given function by monitoring the decay rate of its Legendre expansion coefficients. On the basis of these local regularities, we design and implement an *hp*–adaptive finite element method based on employing discontinuous piecewise polynomials, for the approximation of nonlinear systems of hyperbolic conservation laws. The performance of the proposed adaptive strategy is demonstrated numerically.

1 Introduction

Adaptive finite element methods, capable of approximating solutions to complex multi-dimensional problems with guaranteed error control, are an invaluable computational tool. In general, the construction of an adaptive strategy involves three main steps. The first of these is the derivation of a sharp *a posteriori* error bound for the finite element approximation of the partial differential equation under consideration, which is then used as a stopping criterion to terminate the adaptive algorithm once the desired level of accuracy has been achieved. The second step is the design of an appropriate refinement indicator to identify regions in the computational domain where the error is locally large. Finally, based on the information from the refinement indicator, one may employ a local mesh modification strategy to improve the discretisation within parts of the computational domain where the error is large; this may involve either mesh enrichment (h–refinement) or order variation (p–refinement).

Over the last few decades, considerable progress has been made on both the *a posteriori* error analysis of finite element methods for a wide range of partial differential equations of practical interest, and the theoretical and computational assessment of local refinement indicators; see, for example, [2,5,10,23,26,28] and the references cited therein. We note that once a computable error bound has been established for a particular discretisation of a partial differential equation, the refinement indicator is generally constructed

* Paul Houston and Bill Senior acknowledge the financial support of the EPSRC (GR/N24230).

by simply 'localising' the *a posteriori* bound over an element, or patch of elements. On the other hand, the state of development of 'optimal' mesh modification strategies which are capable of delivering the greatest reduction in the error for the least amount of computational cost, is far less advanced. Indeed, the majority of adaptive finite element software will simply subdivide elements where the local refinement indicator is large, while keeping the polynomial degree fixed at some low value. Clearly, if the analytical solution to the underlying partial differential equation is smooth, or at least locally smooth, then this may not provide the most efficient adaptive strategy. In this case, an enrichment of the polynomial degree (p–refinement) may be much more effective in reducing the error per unit cost. We note that an alternative form of h–refinement, commonly referred to as r–refinement, generally keeps the number of nodes fixed in the mesh, but allows their positions to vary based on the size of a local refinement indicator. Here, we shall not consider r–refinement algorithms.

The aim of this paper is to focus on the design of an automatic mesh modification strategy that is capable of exploiting both local h– and p–refinement. Such general hp–adaptive finite element methods offer greater flexibility and improved efficiency than mesh refinement methods which only incorporate either local mesh subdivision of the computational domain $\Omega \subset \mathbb{R}^d$ with the degree of the approximating polynomial fixed, or global polynomial degree variation on a fixed coarse mesh. Indeed, in recent years there has been tremendous interest in the development of automatic hp–mesh refinement algorithms, see [1,3,6–8,11,14,16–19,23–25,27], for example. The key step in the design of such an adaptive algorithm is the local decision taken on each element κ in the computational mesh as to which refinement strategy (i.e., h-refinement *via* local mesh subdivision or p-refinement by increasing the degree of the local polynomial approximation) should be employed on κ in order to obtain the greatest reduction in the error per unit cost. A number of strategies have been devised to automatically decide which of the two types of refinement to employ. Most of these algorithms implicitly rely on the following result from approximation theory (cf. [4]): suppose that κ is a d–simplex or a d–parallelepiped of diameter h_κ and let $u|_\kappa \in H^{k_\kappa}(\kappa)$, $k_\kappa \geq 0$; then there exists a sequence $z_{p_\kappa}^{h_\kappa}(u)$ in $\mathcal{R}_{p_\kappa}(\kappa)$, $p_\kappa = 1, 2, \ldots$, such that for $0 \leq q \leq k_\kappa$,

$$\|u - z_{p_\kappa}^{h_\kappa}(u)\|_{H^q(\kappa)} \leq C \frac{h_\kappa^{s_\kappa - q}}{p_\kappa^{k_\kappa - q}} \|u\|_{H^{k_\kappa}(\kappa)} \;, \tag{1}$$

where $s_\kappa = \min(p_\kappa + 1, k_\kappa)$ and C is a constant independent of u, h_κ and p_κ, but dependent on k_κ. Here, $\mathcal{R}_{p_\kappa}(\kappa)$ denotes either the set of polynomials of total degree p_κ over κ, or the set of tensor–product polynomials on κ of degree p_κ in each coordinate direction, depending on whether κ is a d–simplex or a d–parallelepiped, respectively.

On the basis of the approximation result (1), hp–adaptive finite element strategies aim to exploit local p-refinement on elements κ where the analytical solution u to the partial differential equation under consideration is *smooth*, i.e., where $k_\kappa > p_\kappa + 1$, for example, and local mesh subdivision on those elements κ where u is nonsmooth, i.e., where $0 \leq k_\kappa \leq p_\kappa + 1$. Thereby, regions in the computational domain where u is locally nonsmooth are isolated from regions of smoothness, thus reducing the influence of singularities/discontinuities as well as making p–refinement more effective. Of course since u is in general unknown analytically, the local Sobolev indices k_κ, and hence the local smoothness of the solution, cannot be determined. Motivated by the lack of precise information about the local regularity of the analytical solution, various algorithms have been developed in the literature with the aim to identify those parts of the computational domain where u may be perceived as being 'smooth' and regions where u is 'nonsmooth'. Below we provide a brief review of existing methods and present an outline of the rest of the paper.

- *Use of a priori information.* For a linear elliptic boundary–value problem with piecewise analytic coefficients, forcing functions and boundary data, on a computational domain Ω with a piecewise analytic boundary surface $\partial\Omega$, the solution will be an analytic function everywhere, except in the neighbourhood of singularities in the data. Thereby, h–refinement may be employed in those elements in the computational domain whose closures contain such singularities, with p–refinement performed elsewhere. This approach has been employed by Owens and co-workers, for example; e.g., see [27], [6].
- *Type–parameter.* In this strategy it is assumed that on each element κ in the computational mesh on Ω, one has a local refinement indicator $\eta_\kappa(u_{h,p}, h_\kappa, p_\kappa)$, which depends on the numerical approximation $u_{h,p}$, the local meshsize h_κ and the local polynomial degree p_κ. Then, assuming that $\eta_\kappa(u_{h,p-1}, h_\kappa, p_\kappa - 1) \neq 0$, the perceived smoothness of the solution may be estimated using the ratio

$$\rho_\kappa = \frac{\eta_\kappa(u_{h,p}, h_\kappa, p_\kappa)}{\eta_\kappa(u_{h,p-1}, h_\kappa, p_\kappa - 1)}\,,$$

  cf. Adjerid *et al.* [1] and Gui & Babuška [11], for example. If $\rho_\kappa \leq \gamma$, $0 < \gamma < 1$, the error is decreasing as the polynomial degree is increased, indicating that p–enrichment should be performed. On the other hand, if $\rho_\kappa > \gamma$ then the element κ is subdivided. The number γ is referred to as a *type–parameter* [11].
- *'Texas 3–step'.* This strategy was first introduced by J.T. Oden and co-workers [18]; here, the smoothness of the solution to the underlying partial differential equation is not directly taken into account. Step 1 involves initialising various parameters, as well as setting intermediate and final error tolerances $\mathtt{TOL}_I$ and $\mathtt{TOL}_F$, respectively. Then, keeping the polynomial degree fixed, in Step 2 the mesh is adaptively h–refined in order to ensure that the error (measured in some appropriate norm) is less than

$\mathtt{TOL}_I$. In the final third step, the mesh is kept fixed, while the local polynomial degrees are increased to achieve the final error tolerance $\mathtt{TOL}_F$. For related work, we refer to the articles [7,17], and the references cited therein.

- *Mesh optimisation strategy.* In this strategy an optimal refinement is determined for each element in the mesh by employing the approximation result (1). More precisely, the left–hand side of (1) is computed for some q by replacing u by a *reference solution* $\hat{u}$. Then, the projector $z_{p_\kappa}^{h_\kappa}(\hat{u})$ is computed on the original element κ with a local polynomial degree $p_\kappa + 1$, as well as on a sequence of finite element spaces corresponding to a local h–refinement of κ that results in the same increase in the number of degrees of freedom as the p–enrichment. The optimal refinement of κ is then chosen to be the one which leads to the smallest projection error; elements in the mesh are then refined based on those that will lead to the greatest decrease in the projection error per degree of freedom. This strategy was first introduced by Rachowicz *et al.* [19]; see also [8] for more recent work.
- *Estimating the decay rate of Legendre expansion coefficients.* Mavriplis [16] proposed determining whether the solution is locally smooth or non-smooth by calculating the decay rate of the Legendre expansion coefficients of the solution. More precisely, writing a_i, $i = 0, \dots,$ to denote the ith Legendre coefficient in a one–dimensional expansion of the solution, it is assumed that
$$a_i \sim C\mathrm{e}^{-\sigma i},$$
where C and σ are constants determined by a least–squares best fit. In [16], p–refinement was employed when $\sigma > 1$; otherwise local mesh subdivision was used.
- *Local regularity estimation.* Here, the idea is to directly approximate the local Sobolev regularity index k_κ on each element κ in the computational mesh; then p–refinement is performed on elements where $k_\kappa > p_\kappa + 1$, otherwise h–refinement is employed. This strategy was first proposed by Ainsworth & Senior [3] in the context of norm control for second–order elliptic problems. In [3], the local Sobolev regularity index k_κ was estimated by employing a local error indicator η_κ which was computed by solving a series of local problems with different polynomial degrees; k_κ could then be extracted by employing local *a priori* error bounds for η_κ. Extensions of this method to linear and nonlinear hyperbolic problems were considered in the series of papers [14,24,25]; as in [3], the strategy employed was based on computing k_κ from a local refinement indicator η_κ computed using different polynomial degrees.

Stimulated by the last two strategies, in this paper we introduce a new technique for assessing local smoothness. By monitoring the decay rate of the sequence of coefficients in the Legendre series expansion of a square–integrable function u, in Section 2 we develop two techniques for directly computing the local Sobolev index of u. The first method is based on applying the Ratio Test to an infinite series involving the Legendre coefficients a_i, while the second relies on the use of the Root Test. The proposed approach has a number of attractions from the computational point of view: firstly, it is entirely general in the sense that it does not depend on the choice of the particular local refinement indicator, and can be applied to any square–integrable function; secondly, it is capable of estimating the local Sobolev regularity of the function u in each coordinate direction separately which is an important feature in the design of anisotropic hp–adaptive finite element algorithms; finally, the technique is computationally inexpensive as it only requires information about the Legendre coefficients of u, which are readily available if a local Legendre basis is used in each element of the computational domain as in a discontinuous Galerkin finite element method. The performance of an automatic hp–adaptive finite element algorithm based on the proposed regularity estimation strategy will be considered in Section 3. Here, we shall be concerned with the hp–version discontinuous Galerkin finite element method applied to nonlinear systems of hyperbolic conservation laws; however, as was indicated above, the technique is more generally applicable.

2 Regularity estimation

In this section we consider the estimation of the Sobolev regularity of a given function $u : \Omega \to \mathbb{R}$, where Ω is a bounded open subset of the real line; without loss of generality, we select $\Omega = (-1, 1)$. Extensions to higher dimensions follow analogously by a tensor product construction; this will be discussed in Section 2.3. We begin by first recalling some basic properties of Legendre polynomials defined on $(-1, 1)$; for further details, we refer to Schwab [21], and the references cited therein.

Suppose that $u \in L_2(-1, 1)$; then u can be expanded into the Legendre series

$$u(x) = \sum_{i=0}^{\infty} a_i L_i(x) \qquad \text{with} \qquad a_i = \frac{2i+1}{2} \int_{-1}^{1} u(x) L_i(x) \, \mathrm{d}x \,, \tag{2}$$

which converges in (the norm of) $L_2(-1, 1)$. Here $L_i(x)$ denotes the Legendre polynomial in x of degree $i \geq 0$. Due to the orthogonality properties of Legendre polynomials in the inner product of $L_2(-1, 1)$, the following Parseval's identity holds (cf. Schwab [21], Lemma 3.10, p.71):

$$\int_{-1}^{1} |u(x)|^2 \, \mathrm{d}x = \sum_{i=0}^{\infty} |a_i|^2 \frac{2}{2i+1} \,. \tag{3}$$

If u possesses additional regularity, then a stronger result can be proved. Let us assume, for example, that u belongs to the weighted Sobolev space

$H^k_w(-1,1)$ of integer index $k \geq 0$; i.e., suppose that

$$\begin{aligned}\|u\|^2_{H^k_w(-1,1)} &= \sum_{j=0}^{k} |u|^2_{H^j_w(-1,1)} \\ &\equiv \sum_{j=0}^{k} \int_{-1}^{1} \left|D^{(j)}u(x)\right|^2 (1-x^2)^j \,\mathrm{d}x < \infty\,;\end{aligned}$$

then,

$$|u|^2_{H^k_w(-1,1)} = \sum_{i=k}^{\infty} |a_i|^2 \frac{2}{2i+1} \frac{(i+k)!}{(i-k)!}\,. \tag{4}$$

We note that $k! = \Gamma(k+1)$ for integer $k > 0$, where Γ is the Gamma function defined, for $x > 0$, by

$$\Gamma(x) = \int_0^\infty \mathrm{e}^{-t} t^{x-1} \,\mathrm{d}t\,.$$

Further, let

$$\lceil k \rceil = \begin{cases} [k]+1 & \text{if } k \text{ is fractional,} \\ k & \text{if } k \text{ is integer.} \end{cases}$$

Motivated by the identity (4), for fractional $k > 0$ we define the weighted Sobolev space $H^k_w(-1,1)$ as the set of all u in $H^{[k]}_w(-1,1)$ such that

$$|u|^2_{H^k_w(-1,1)} \equiv \sum_{i=\lceil k \rceil}^{\infty} |a_i|^2 \frac{2}{2i+1} \frac{\Gamma(i+k+1)}{\Gamma(i-k+1)} < \infty\,, \tag{5}$$

and let

$$\|u\|^2_{H^k_w(-1,1)} = \|u\|^2_{H^{[k]}_w(-1,1)} + |u|^2_{H^k_w(-1,1)}\,.$$

We note that allowing k to be integer in (5) we obtain (4). Therefore,

$$|u|^2_{H^k_w(-1,1)} = \sum_{\lceil k \rceil}^{\infty} |a_i|^2 \frac{2}{2i+1} \frac{\Gamma(i+k+1)}{\Gamma(i-k+1)} < \infty \qquad \forall k \geq 0\,. \tag{6}$$

Let $\tau = k - [k]$; for fractional $k > 0$ we then have $\tau \in (0,1)$. The logarithmic convexity property

$$\begin{aligned}\frac{\Gamma(i+k+1)}{\Gamma(i-k+1)} &= \frac{\Gamma(i+[k]+\tau+1)}{\Gamma(i-[k]-\tau+1)} \\ &\leq \left(\frac{\Gamma(i+[k]+1)}{\Gamma(i-[k]+1)}\right)^{1-\tau} \left(\frac{\Gamma(i+[k]+2)}{\Gamma(i-[k])}\right)^{\tau}, \quad i \geq [k]\,,\end{aligned}$$

and Hölder's inequality then imply that, for fractional $k > 0$ and any u in $H_w^{[k+1]}(-1,1)$,

$$
\begin{aligned}
|u|_{H_w^k(-1,1)} &= \left(\sum_{i=[k]+1}^{\infty} |a_i|^2 \frac{2}{2i+1} \frac{\Gamma(i+k+1)}{\Gamma(i-k+1)} \right)^{\frac{1}{2}} \\
&\leq \left(\sum_{i=[k]+1}^{\infty} |a_i|^2 \frac{2}{2i+1} \frac{\Gamma(i+[k]+1)}{\Gamma(i-[k]+1)} \right)^{\frac{1-\tau}{2}} \left(\sum_{i=[k]+1}^{\infty} |a_i|^2 \frac{2}{2i+1} \frac{\Gamma(i+[k]+2)}{\Gamma(i-[k])} \right)^{\frac{\tau}{2}} \\
&\leq |u|^{1-\tau}_{H_w^{[k]}(-1,1)} |u|^{\tau}_{H_w^{[k+1]}(-1,1)} \, ;
\end{aligned}
$$

thus, also

$$
\|u\|_{H_w^k(-1,1)} \leq 2^{(1-\tau)/2} \|u\|^{1-\tau}_{H_w^{[k]}(-1,1)} \|u\|^{\tau}_{H_w^{[k+1]}(-1,1)} \, ,
$$

for any $u \in H_w^{[k+1]}(-1,1)$. Hence, for any fractional $k > 0$,

$$
H_w^k(-1,1) = [H_w^{[k]}(-1,1), H_w^{[k]+1}(-1,1)]_\tau \, , \qquad 0 < \tau < 1 \, ,
$$

where $[\cdot,\cdot]_\tau$ denotes the functor of the K-method of function space interpolation with $\tau = k - [k] \in (0,1)$.

In the following sections, we develop two techniques for estimating the Sobolev index of a function $u \in L_2(-1,1)$ by monitoring the decay of the sequence of coefficients $(|a_i|^2/(2i+1))_{i\geq 0}$ in Parseval's identity (3). The first technique is based on the application of the Ratio Test, while the second relies on the use of the Root Test. For the sake of simplicity of presentation, we shall suppose throughout that none of the coefficients a_i, $i \geq 0$, is equal to zero. For certain classes of functions, — for odd or even functions defined on the interval $[-1,1]$, for example, — it may turn out that some of the Legendre expansion coefficients a_i, $i \geq 0$, appearing in (2) are zero. In this case the zero coefficients must first be 'filtered out' of the sequence $(a_i)_{i\geq 0}$ before the algorithms presented in Sections 2.1 and 2.2 can be applied.

2.1 The Ratio Test Algorithm

Suppose that $u \in L_2(-1,1)$ and let $(a_i)_{i\geq 0}$ denote the set of Legendre coefficients of u. As

$$
\mathcal{S} = \sum_{i=0}^{\infty} |a_i|^2 \frac{2}{2i+1} < \infty \, , \tag{7}
$$

cf. (3), it follows that the sequence $(b_i)_{i\geq 1}$, where

$$
b_i = \left(\frac{a_i}{a_{i-1}} \right)^2 \frac{2i-1}{2i+1} \, , \qquad i \geq 1 \, , \tag{8}
$$

is bounded. Let us suppose that

$$\theta = \lim_{i\to\infty} b_i = \lim_{i\to\infty} \left(\frac{a_i}{a_{i-1}}\right)^2 \frac{2i-1}{2i+1} \tag{9}$$

exists. According to the Ratio Test (cf. [9], for example) $\theta \in (0,1]$, for otherwise $\mathcal{S}$ would diverge, contradicting (7). The cases $\theta \in (0,1)$ and $\theta = 1$ will be discussed below separately.

Case 1. Let us first suppose that $\theta \in (0,1)$. We recall that by Stirling's formula

$$\Gamma(n+1) \asymp \sqrt{2\pi}\, n^{n+1/2} \exp\left(-n + \frac{1}{12n}\right) \qquad \text{as } n \to \infty\,;$$

thereby,

$$\lim_{i\to\infty} \left(\frac{a_i}{a_{i-1}}\right)^2 \frac{2i-1}{2i+1} \frac{\Gamma(i+k+1)}{\Gamma(i-k+1)} \frac{\Gamma(i-k)}{\Gamma(i+k)} = \theta \lim_{i\to\infty} \frac{1+(k/i)}{1-(k/i)} = \theta$$

for all $k \geq 0$. Consequently, by the Ratio Test, the series on the right–hand side of (6) is convergent for all $k \geq 0$, which implies that

$$u \in \bigcap_{k\geq 0} H_w^k(-1,1)\,;$$

in particular, $u \in C^\infty(-1,1)$. In other words, if $\theta \in (0,1)$, the function u is regular in $(-1,1)$.

Case 2. Now we consider the case when $\theta = 1$. In this case, $\lim_{i\to\infty} b_i = 1$ (i.e., $\lim_{i\to\infty}(1-b_i) = 0$), where b_i is defined by (8). Let us suppose that there exists a positive real number ℓ such that

$$\ell = \frac{1}{2} \lim_{i\to\infty} i(1-b_i)\,. \tag{10}$$

The existence of this limit then implies that $\lim_{i\to\infty} b_i$ exists and $\lim_{i\to\infty} b_i = \theta = 1$. Next we show that, necessarily, $\ell \geq 1/2$. We begin by noting that

$$\ell = \frac{1}{2} i(1-b_i) + o(1) \qquad \text{as } i \to \infty\,.$$

Hence,

$$b_i = 1 - \frac{2\ell}{i} + o\left(\frac{1}{i}\right) \qquad \text{as } i \to \infty\,. \tag{11}$$

By the Gauss Test (cf. Douglass [9], for example), we must have $2\ell \geq 1$, for otherwise the series $\mathcal{S}$ would diverge, contradicting the basic hypothesis that $u \in L_2(-1,1)$. We shall first consider the case when $\ell > 1/2$. Let $k \in [0, \ell - 1/2)$; then, by virtue of Stirling's formula, we get

$$\begin{aligned}\left(\frac{a_i}{a_{i-1}}\right)^2 \frac{2i-1}{2i+1} \frac{\Gamma(i+k+1)}{\Gamma(i-k+1)} \frac{\Gamma(i-k)}{\Gamma(i+k)} \\ &= b_i \frac{\Gamma(i+k+1)}{\Gamma(i-k+1)} \frac{\Gamma(i-k)}{\Gamma(i+k)} \\ &= \left(1 - \frac{2\ell}{i} + o\left(\frac{1}{i}\right)\right)\left(1 + \frac{2k}{i} + o\left(\frac{1}{i}\right)\right) \\ &= 1 - \frac{2(\ell-k)}{i} + o\left(\frac{1}{i}\right), \qquad \text{as } i \to \infty .\end{aligned}$$

As $k \in [0, \ell - 1/2)$, it follows that $2(\ell - k) > 1$, and therefore by the Gauss Test,

$$\sum_{i=\lceil k \rceil}^{\infty} |a_i|^2 \frac{2}{2i+1} \frac{\Gamma(i+k+1)}{\Gamma(i-k+1)} < \infty .$$

Hence, $u \in H_w^k(-1,1)$ for all $k \in [0, \ell - 1/2)$, i.e.,

$$u \in H_w^{\ell-1/2-\varepsilon}(-1,1), \qquad 0 < \varepsilon \leq \ell - \frac{1}{2} .$$

The case of $\ell = 1/2$ formally returns our basic hypothesis that $u \in L_2(-1,1)$ and is therefore of no practical significance.

Since the weight function $x \mapsto (1 - x^2)$ belongs to $C^\infty(-1,1)$ and is positive on $(-1,1)$, we deduce that if $u \in H_w^{\ell-1/2-\varepsilon}(-1,1)$ then

$$u \in H_{\mathrm{loc}}^{\ell-1/2-\varepsilon}(-1,1), \qquad 0 < \varepsilon \leq \ell - \frac{1}{2} .$$

We summarise our findings in the following pseudocode in Fig. 1.

`Step 1` `Given a function` $u \in L_2(-1,1)$, `expand it into a Legendre series (2) with coefficients` a_i, $i \geq 0$.
`Step 2` `Define` b_i, $i \geq 1$, `by (8) and compute` $\theta = \lim_{\to\infty} b_i$.
`Step 3` `If` $\theta \in (0,1)$, `then` $u \in C^\infty(-1,1)$. `STOP`
`Step 4` `Else, if the limit` $\ell = \frac{1}{2}\lim_{i\to\infty} i(1-b_i)$ `exists and` $\ell > 1/2$, `then` $u \in H_w^{\ell-1/2-\varepsilon}(-1,1)$, $0 < \varepsilon \leq \ell - 1/2$. `STOP`
`Step 5` `Else` $u \in L_2(-1,1)$. `STOP`

Fig. 1. The Ratio Test Algorithm

2.2 The Root Test Algorithm

Let us again suppose that $u \in L_2(-1,1)$; then it follows from (3) that the series $\mathcal{S}$ in (7) converges. Consequently, the sequence $(c_i)_{i\geq 1}$, where c_i is defined by

$$c_i = \left(|a_i|^2 \frac{2}{2i+1}\right)^{1/i}, \qquad i \geq 1, \tag{12}$$

is bounded. Let us define

$$\theta = \overline{\lim}_{i\to\infty} c_i = \overline{\lim}_{i\to\infty} \left(|a_i|^2 \frac{2}{2i+1}\right)^{1/i}. \tag{13}$$

According to the Root Test (cf. [9], for example) $\theta \in (0,1]$, for otherwise $\mathcal{S}$ would diverge, contradicting (7). As in the previous section, the cases $\theta \in (0,1)$ and $\theta = 1$ will be discussed below separately.

Case 1. If $\theta \in (0,1)$, then by Stirling's formula we have

$$\overline{\lim}_{i\to\infty} \left(|a_i|^2 \frac{2}{2i+1} \frac{\Gamma(i+k+1)}{\Gamma(i-k+1)}\right)^{1/i} = \theta \lim_{i\to\infty} (i^{2k})^{1/i} = \theta$$

for all $k \geq 0$. Thereby, the series on the right–hand side of (6) is convergent for all $k \geq 0$, which implies that

$$u \in \bigcap_{k\geq 0} H^k_w(-1,1).$$

Hence, for $\theta \in (0,1)$, $u \in C^\infty(-1,1)$ and is therefore regular in $(-1,1)$.

Case 2. Now, let $\theta = 1$ and suppose that there exists a positive real number ℓ such that

$$\ell = \lim_{i\to\infty} \frac{\log\left(\frac{2i+1}{2|a_i|^2}\right)}{2\log i}. \tag{14}$$

We shall show that, necessarily, $\ell \geq 1/2$; to this end, we note that (14) yields

$$\ell = \frac{\log\left(\frac{2i+1}{2|a_i|^2}\right)}{2\log i} + o(1) \qquad \text{as } i \to \infty.$$

Thereby,

$$\log\left(|a_i|^2 \frac{2}{2i+1}\right)^{1/i} = -\frac{2\ell \log i}{i} + o\left(\frac{\log i}{i}\right), \qquad i \to \infty. \tag{15}$$

The Logarithmic Gauss Test[1] implies that $2\ell \geq 1$; otherwise the series $\mathcal{S}$ would diverge, contradicting the basic hypothesis that $u \in L_2(-1,1)$. Let us first consider the case when $\ell > 1/2$; given $k \in [0, \ell - 1/2)$, using equation (15) we deduce that

$$\left(|a_i|^2 \frac{2}{2i+1}\right)^{1/i} = \exp\left\{-\frac{2\ell \log i}{i} + o\left(\frac{\log i}{i}\right)\right\}, \qquad i \to \infty .$$

Hence, by Stirling's formula,

$$\begin{aligned}\left(|a_i|^2 \frac{2}{2i+1} \frac{\Gamma(i+k+1)}{\Gamma(i-k+1)}\right)^{1/i} \\ &= \exp\left\{-\frac{2\ell \log i}{i} + o\left(\frac{\log i}{i}\right)\right\} \exp\left\{\frac{2k \log i}{i} + o\left(\frac{\log i}{i}\right)\right\} \\ &= \exp\left\{-\frac{2(\ell - k)\log i}{i} + o\left(\frac{\log i}{i}\right)\right\} .\end{aligned}$$

Given that $k \in [0, \ell - 1/2)$, it follows that $2(\ell - k) > 1$, and therefore by the Logarithmic Gauss Test,

$$\sum_{i=[k]}^{\infty} |a_i|^2 \frac{2}{2i+1} \frac{\Gamma(i+k+1)}{\Gamma(i-k+1)} < \infty .$$

Consequently, $u \in H^k_w(-1,1)$ for all $k \in [0, \ell - 1/2)$, i.e.,

$$u \in H_w^{\ell - 1/2 - \varepsilon}(-1,1), \qquad 0 < \varepsilon \leq \ell - \frac{1}{2} .$$

As before, the case of $\ell = 1/2$ formally returns our basic hypothesis that $u \in L_2(-1,1)$.

Finally, since the weight function $x \mapsto (1-x^2)$ belongs to $C^\infty(-1,1)$ and is positive on $(-1,1)$, we again deduce that if $u \in H_w^{\ell-1/2-\varepsilon}(-1,1)$ then

$$u \in H_{\mathrm{loc}}^{\ell - 1/2 - \varepsilon}(-1,1), \qquad 0 < \varepsilon \leq \ell - \frac{1}{2} .$$

We summarise our findings in the pseudocode in Fig. 2.

From the discussion in this section and the previous one, we see that the local Sobolev regularity of a square-integrable function u may be determined from the formulas for ℓ given by equations (10) and (14). In the next section, we present a practical algorithm based on these theoretical results; in particular, we discuss the extension of our results to higher space dimensions.

[1] The Logarithmic Gauss Test: Suppose that $\sum_{i=0}^{\infty} \alpha_i$ is a series with positive entries α_i, $i \geq 0$, and assume that

$$\log(\alpha_i)^{1/i} = -\frac{p \log i}{i} + o\left(\frac{\log i}{i}\right), \qquad i \to \infty .$$

If $p < 1$, then the series is divergent; if $p > 1$ the series is convergent; if $p = 1$ the test is indecisive. The proof is analogous to that of the classical Gauss test [9].

Step 1 Given a function $u \in L_2(-1,1)$, expand it into a Legendre series (2) with coefficients a_i, $i \geq 0$.

Step 2 Define c_i, $i \geq 1$, by (12) and compute $\theta = \overline{\lim}_{i\to\infty} \left(|a_i|^2 \frac{2}{2i+1}\right)^{1/i}$.

Step 3 If $\theta \in (0,1)$, then $u \in C^\infty(-1,1)$. STOP

Step 4 Else, if the limit

$$\ell = \lim_{i\to\infty} \frac{\log\left(\frac{2i+1}{2|a_i|^2}\right)}{2\log i}$$

exists and $\ell > 1/2$, then $u \in H_w^{\ell-1/2-\varepsilon}(-1,1)$, $0 < \varepsilon \leq \ell - 1/2$. STOP

Step 5 Else $u \in L_2(-1,1)$. STOP

Fig. 2. The Root Test Algorithm

2.3 Practical implementation

Based on the analysis presented in Sections 2.1 and 2.2, we see that there are essentially two cases which must be considered when determining the regularity of u by monitoring the decay of its Legendre expansion coefficients: either u is regular in $(-1,1)$ corresponding to the case when $\theta \in (0,1)$, cf. (9) and (13) for the Ratio and Root Test, respectively; or $\theta = 1$, indicating that u has finite Sobolev regularity. Of course, all of these results are asymptotic, in the sense that they only hold as i tends to infinity. Thereby, in practice, rather than monitoring θ as i increases, for a given i, $i \geq 0$, we predict the regularity on the basis of the formulas for ℓ given in equations (10) and (14). More precisely, let us suppose that we have computed the first $k+1$ Legendre coefficients of a function $u \in L_2(-1,1)$, i.e., we have the set $\{a_0, a_1, \ldots, a_k\}$. Then, we estimate the regularity of u by employing one of the formulas

$$\ell_k = \frac{i(1-b_k)}{1+b_k}, \quad k \geq 1; \qquad \text{or} \qquad \ell_k = \frac{\log\left(\frac{2k+1}{2|a_k|^2}\right)}{2\log k}, \quad k \geq 2; \tag{16}$$

depending on whether the Ratio or Root Test is used, respectively; here, b_k, $k \geq 0$, is defined by (8). In each case, u is then predicted to belong to $H_w^{\ell_k-1/2-\varepsilon}(-1,1)$, $0 < \varepsilon \leq \ell_k - 1/2$. If u is smooth on $(-1,1)$, then in practice the sequence (ℓ_k) will simply grow as k is increased; indeed, if $u \in C^\infty(-1,1)$, then $\lim_{k\to\infty} \ell_k = +\infty$.

Finally, we remark that for odd and even coefficients, the value of ℓ_k may oscillate corresponding to the fact that the odd and even modes of the function u decay at different rates; in this case, the estimated regularity of u is taken to be equal to $\min(\ell_k, \ell_{k-1}) - 1/2 - \varepsilon$.

We end this section by considering some extensions of the analysis presented in Sections 2.1 and 2.2.

Boundary singularities Since the weight function $x \mapsto (1-x^2)$ vanishes at the end points of the interval $(-1,1)$, if $u \in H_w^s(-1,1)$ then $H_{\mathrm{loc}}^s(-1,1)$, but it need not be true that $u \in H^s(-1,1)$; indeed, due to the embedding of $H^s_w(-1,1)$ into $H^{s/2}(-1,1)$ the index of standard (unweighted) Sobolev regularity of a function $(-1,1)$ may be only half of its index of weighted Sobolev regularity. Given a function $u \in H^s_w(-1,1)$ (which, thereby, also belongs to $H^s_{\mathrm{loc}}(-1,1)$), it is fairly easy to assess whether or not u belongs to $H^s(-1,1)$: if the regularities predicted by either of our two algorithms for the functions u and $(1-x^2)u$ differ, then u possesses a dominant singularity at $x=-1$ or $x=1$; thereby, the index of standard unweighted Sobolev regularity of u on $(-1,1)$ is half of the index of w-weighted Sobolev space regularity on $(-1,1)$ (and also, half of the index of unweighted *local* Sobolev regularity on $(-1,1)$) predicted by either the Ratio Test or the Root Test Algorithm. Otherwise, if the regularities of u and $(1-x^2)u$ predicted by either of our algorithms coincide, then the dominant singularity of u lies in $(-1,1)$ and therefore the index of w-weighted Sobolev regularity of u on $(-1,1)$ will coincide with the index of standard unweighted Sobolev space regularity of u on $(-1,1)$.

Higher–dimensional space Both techniques can be employed to estimate the regularity of a function $u : \Omega \to \mathbb{R}$, where Ω is a bounded open subset of $\mathbb{R}^n$, $n \geq 1$, provided that Ω is the image of the reference domain $(-1,1)^n$ under a bijective C^∞ mapping. For simplicity, let us consider the case when $n=2$ and $\Omega=(-1,1)^2$; extensions to higher dimensions follow analogously. A function $u \in L_2(\Omega)$ can be expanded into the tensor product Legendre series

$$u(x,y) = \sum_{i,j=0}^{\infty} a_{i,j} L_i(x) L_j(y),$$

with

$$a_{i,j} = \frac{2i+1}{2}\,\frac{2j+1}{2} \int_\Omega u(x,y) L_i(x) L_j(y)\,\mathrm{d}x\,\mathrm{d}y\,,$$

which converges in the $L_2(\Omega)$–norm. As in the one–dimensional case the following Parseval's identity holds:

$$\int_\Omega |u(x,y)|^2\,\mathrm{d}x\,\mathrm{d}y = \sum_{i=0}^{\infty} |a_{i,j}|^2 \frac{2}{2i+1}\,\frac{2}{2j+1}\,.$$

Moreover, if we suppose that u belongs to the anisotropic weighted Sobolev space $H^{k_x,k_y}_w(\Omega)$ with integer indices k_x, k_y; i.e.,

$$\begin{aligned}\|u\|^2_{H^{k_x,k_y}_w(\Omega)} &= \sum_{l=0}^{k_x}\sum_{m=0}^{k_y} |u|^2_{H^{l,m}_w(\Omega)}\\ &\equiv \sum_{l=0}^{k_x}\sum_{m=0}^{k_y} \int_\Omega \left|D^{(l,m)}u(x,y)\right|^2 (1-x^2)^l(1-y^2)^m\,\mathrm{d}x\,\mathrm{d}y < \infty\,;\end{aligned}$$

then

$$|u|^2_{H_w^{k_x,k_y}(\Omega)} = \sum_{i=k_x}^{\infty} \sum_{j=k_y}^{\infty} |a_{i,j}|^2 \frac{2}{2i+1} \frac{2}{2j+1} \frac{\Gamma(i+k_x+1)}{\Gamma(i-k_x+1)} \frac{\Gamma(j+k_y+1)}{\Gamma(j-k_y+1)} . \quad (17)$$

The extension to the case when k_x, k_y are not integers follows analogously as outlined at the beginning of Section 2 in the one-dimensional case.

The Ratio Test may now be applied as in Section 2.1 in each coordinate direction by considering successive terms in the summation on the right–hand side of (17) with respect to i for j fixed, then for j with i fixed. The application of the Root Test is as follows: let us first suppose that we wish to estimate k_x, i.e., the regularity of u in the x–direction. Then we calculate the summation over j with $k_y \equiv 0$; thereby (17) becomes

$$|u|^2_{H_w^{k_x,k_y}(\Omega)} = \sum_{i=k_x}^{\infty} |\hat{a}_i|^2 \frac{2}{2i+1} \frac{\Gamma(i+k_x+1)}{\Gamma(i-k_x+1)} , \quad (18)$$

where

$$|\hat{a}_i|^2 = \sum_{j=k_y}^{\infty} |a_{i,j}|^2 \frac{2}{2j+1} ,$$

for $i \geq 0$. The one–dimensional algorithm developed in Section 2.2 may now be applied directly to (18) in order to estimate k_x. Similarly, k_y may be determined by performing a summation over i.

2.4 Numerical experiments

In this section we present some numerical examples to illustrate the performance of the proposed regularity estimation algorithm based on employing the Root Test. Here, we shall not consider the Ratio Test algorithm developed in Section 2.1, as in general we found the practical performance of this method to be inferior to that of the Root Test.

Example 1 In this first example, we consider the function

$$u(x) = \begin{cases} 0, & -1 \leq x < \beta, \\ (x-\beta)^{\alpha}, & \beta \leq x \leq 1, \end{cases}$$

defined on the domain $(-1, 1)$, where $\alpha \geq 0$ and $-1 < \beta < 1$; thereby, $u \in H^{\alpha+1/2-\varepsilon}(-1,1)$, $\varepsilon > 0$, for any $\beta \in (-1,1)$.

In Figs. 3(a) & (b), we plot the actual and predicted regularity of u for $\alpha = 0$ and $\beta = 0, -1/10$, respectively. Here, we see that the regularity of u is slightly over–predicted in each case, with the estimated Sobolev index slowly tending to the true value as more Legendre coefficients are employed. We note that the algorithm is more accurate when the discontinuity in u lies in the

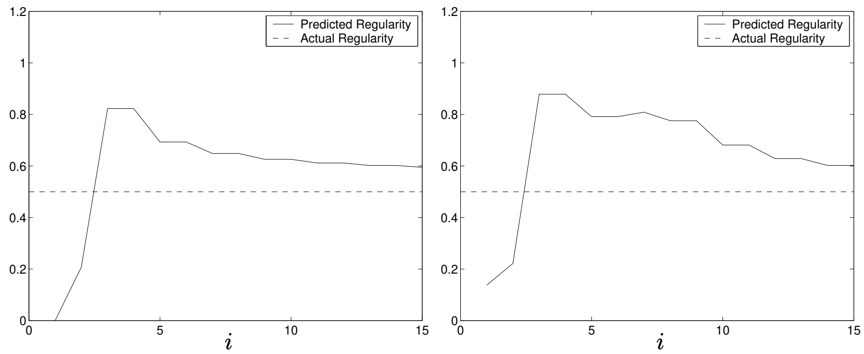

(a) (b)

Fig. 3. Example 1. Regularity estimation when $\alpha = 0$ and: (a) $\beta = 0$; (b) $\beta = -1/10$

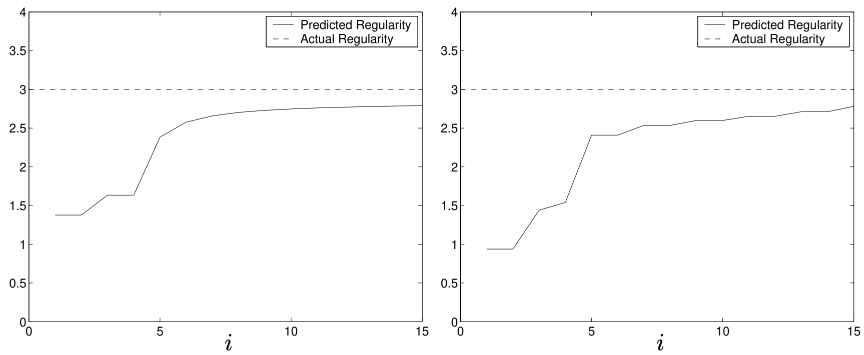

(a) (b)

Fig. 4. Example 1. Regularity estimation when $\alpha = 5/2$ and: (a) $\beta = 0$; (b) $\beta = -1/10$

middle of the domain. Moreover, we observe that a 'reasonable' prediction concerning the relative smoothness of u may already be made using only the first few coefficients; this will be particularly important for the application of this approach in the design of hp–adaptive finite element methods. Finally, in Figs. 4(a) & (b) we show the actual and predicted regularity of u for $\alpha = 5/2$ and $\beta = 0, -1/10$, respectively. In this case, we see that the actual regularity of u is now slightly under–predicted, though, as before the algorithm is more accurate when the singularity in u is located at $x = 0$.

Example 2 In this example, we investigate the performance of the Root Test algorithm for a function u which has a singularity located at the end

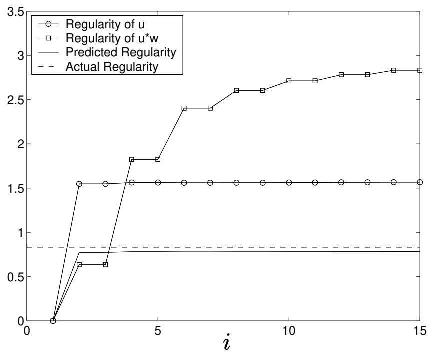

Fig. 5. Example 2. Regularity estimation when $\alpha = 1/3$

points of the domain $\Omega = (-1,1)$. Thus we let

$$u(x) = (1-x^2)^\alpha,$$

where $\alpha > 0$ is not an integer; in this case, $u \in H^{\alpha+1/2-\varepsilon}(-1,1)$, $\varepsilon > 0$.

From Fig. 5 we see that the regularity of u for $\alpha = 1/3$ predicted by the Root Test Algorithm is $k \approx 1.56$. If we now apply the Root Test Algorithm to estimate the regularity of $(1-x^2)u$, then the sequence of predicted Sobolev indices for $(1-x^2)u$ tends to 3. Hence, we have a sizable mismatch between the predicted indices of w-weighted Sobolev space regularities of u and $(1-x^2)u$, showing that u has a dominant singularity at the endpoints of the domain $\bar{\Omega}$, cf. Section 2.3. Consequently, the predicted number $k \approx 1.56$ is the index of w-weighted Sobolev space regularity in $H^k_w(-1,1)$ rather than the index of standard (unweighted) Sobolev space regularity in $H^k(-1,1)$. By using the embedding of $H^k_w(-1,1)$ into $H^{k/2}(-1,1)$, we conclude that the index of standard (unweighted) Sobolev regularity is approximately $1.56/2 \approx 0.78$; this is very close to the actual value of ≈ 0.83.

Example 3 Here, we consider the performance of the regularity estimation algorithm for a function $u : \Omega \mapsto \mathbb{R}$, where Ω is an open quadrilateral domain in $\mathbb{R}^2$ with nonempty intersection with the line $x = 0$. More precisely, we let

$$u(x,y) = \begin{cases} \cos(\pi y/2)\,, & \text{for } x < 0\,, \\ \cos(\pi y/2) + x^\alpha\,, & \text{for } x \geq 0\,, \end{cases}$$

where α is a nonnegative constant; consequently, u belongs to the Sobolev space $H^{\alpha+1/2-\varepsilon}(\Omega)$, for any $\varepsilon > 0$. In order to test the accuracy of the Root Test Algorithm when the domain Ω is not an affine image of the reference domain $(-1,1)^2$, we applied the Algorithm to the pull-back of u on the reference domain $(-1,1)^2$. The predicted regularities, when Ω is each of the quadrilaterals in Fig. 6, are shown in Fig. 7. We observe that the Root Test

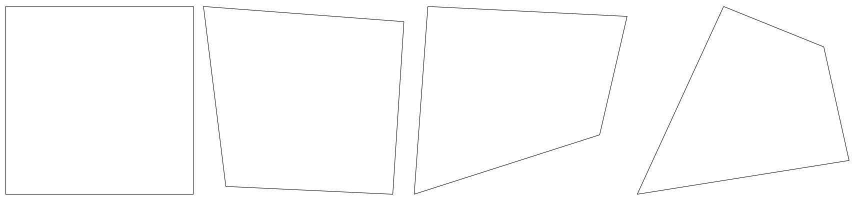

Fig. 6. Example 3. Quadrilateral domains Ω employed

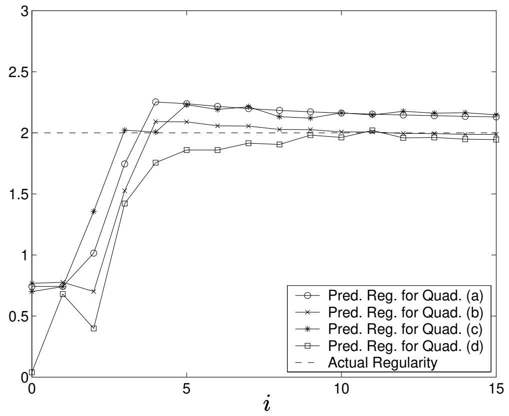

Fig. 7. Example 3. Regularity estimation when $\alpha = 3/2$

Algorithm provides an accurate prediction of the regularity of u using only the first few Legendre expansion coefficients; moreover, we see that the accuracy of the predicted regularity is fairly insensitive to the distortion of Ω and thereby to the lack of affineness of the mapping from the reference domain $(-1,1)^2$ to the computational domain Ω.

Example 4 In this final example we consider the function

$$u(x, y) = \arctan(50(x^3 - x^2 - 1 - y))$$

on $\Omega = (-3, 4) \times (-6, 6)$. In Fig. 8 we show the predicted regularities of u in the x– and y–coordinate directions, denoted by k_x and k_y, respectively, computed on a uniform 65×65 mesh consisting of quadrilateral elements using discontinuous piecewise bicubic polynomials. For clarity, we simply plot $\min(k_x, p)$ and $\min(k_y, p)$, where p is the polynomial degree, i.e., $p = 3$. We clearly see that the Root Test Algorithm not only accurately predicts the location of the transition layer present in u, but also the local anisotropy of the regularities of u. Indeed, we observe that k_x is small in the vertical

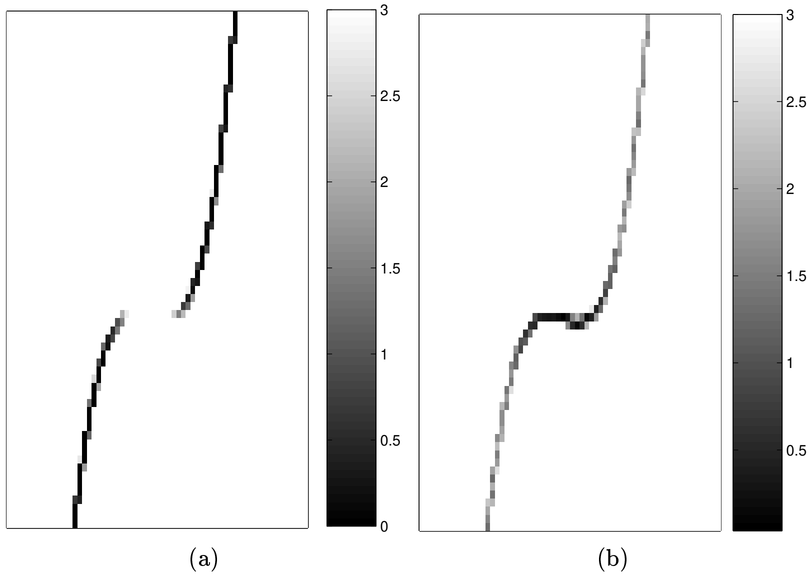

Fig. 8. Example 4. Regularity estimation: (a) $\min(k_x, p)$; (b) $\min(k_y, p)$

sections of the steep internal layer in u and larger in the horizontal part of the layer, with the opposite behaviour in k_y. This feature of our regularity estimation strategy will be of great practical importance in the design of anisotropic hp–adaptive finite element methods; though, this is beyond the scope of the present paper.

3 Adaptive hp–DGFEM

In this section, we now consider the performance of the proposed regularity estimation strategy in the design of an automatic hp–adaptive algorithm for the discontinuous Galerkin finite element method (DGFEM, for short) applied to nonlinear systems of hyperbolic conservation laws.

3.1 Model problem and discretisation

Given a bounded open polyhedral domain Ω in $\mathbb{R}^n$, $n \geq 1$, with boundary $\partial\Omega$, we consider the following problem: find $\mathbf{u} : \Omega \to \mathbb{R}^m$, $m \geq 1$, such that

$$\mathrm{div}\mathcal{F}(\mathbf{u}) = 0 \quad \text{in } \Omega, \tag{19}$$

where, $\mathcal{F} : \mathbb{R}^m \to \mathbb{R}^{m \times n}$ is continuously differentiable. We assume that the system of conservation laws (19) may be supplemented by appropriate initial/boundary conditions. For example, assuming that

$$B(\mathbf{u},\nu) := \sum_{i=1}^{n} \nu_i \nabla_{\mathbf{u}} \mathcal{F}_i(\mathbf{u})$$

has m real eigenvalues and a complete set of linearly independent eigenvectors for all $\nu = (\nu_1, \dots, \nu_n) \in \mathbb{R}^n$, then at inflow/outflow boundaries, we set $B^-(\mathbf{u},\mathbf{n})(\mathbf{u}-\mathbf{g}) = \mathbf{0}$, where $\mathbf{n}$ denotes the unit outward normal vector to $\partial\Omega$, $B^-(\mathbf{u},\mathbf{n})$ is the negative part of $B(\mathbf{u},\mathbf{n})$ and $\mathbf{g}$ is a (given) real–valued function.

To formulate the discontinuous Galerkin finite element approximation of (19), we first need to introduce some notation. Let $\mathcal{T}_h = \{\kappa\}$ be a regular or 1–irregular subdivision of Ω into open element domains κ; here h is a piecewise constant mesh function with $h(\mathbf{x}) = \mathrm{diam}(\kappa)$ when $\mathbf{x}$ is in element κ. We shall suppose that the family of subdivisions $\mathcal{T}_h$ is shape–regular and that each $\kappa \in \mathcal{T}_h$ is a smooth bijective image of a fixed reference element $\hat{\kappa}$, that is, $\kappa = F_\kappa(\hat{\kappa})$ for all $\kappa \in \mathcal{T}_h$ where $\hat{\kappa}$ is either the open unit simplex $\hat{\kappa}_{\mathrm{S}}$ or the open unit hypercube $\hat{\kappa}_{\mathrm{C}}$ in $\mathbb{R}^n$. On the reference element $\hat{\kappa}$ we define spaces of polynomials of degree $p \geq 1$ as follows:

$$\mathcal{Q}_p = \mathrm{span}\left\{\hat{x}^\alpha : 0 \leq \alpha_i \leq p,\ \ 1 \leq i \leq n\right\}, \quad \mathcal{P}_p = \mathrm{span}\left\{\hat{x}^\alpha : 0 \leq |\alpha| \leq p\right\}.$$

To each $\kappa \in \mathcal{T}_h$ we assign an integer $p_\kappa \geq 1$; collecting the p_κ and F_κ in the vectors $\mathbf{p} = \{p_\kappa : \kappa \in \mathcal{T}_h\}$ and $\mathbf{F} = \{F_\kappa : \kappa \in \mathcal{T}_h\}$, respectively, we introduce the finite element space

$$\begin{aligned} S^{\mathbf{p}}(\Omega,\mathcal{T}_h,\mathbf{F}) = \{\mathbf{u} \in [L_2(\Omega)]^m \ : \ & \mathbf{u}|_\kappa \circ F_\kappa \in [\mathcal{Q}_{p_\kappa}]^m \ \text{ if } F_\kappa^{-1}(\kappa) = \hat{\kappa}_{\mathrm{C}} \\ \text{and} \quad & \mathbf{u}|_\kappa \circ F_\kappa \in [\mathcal{P}_{p_\kappa}]^m \ \text{ if } F_\kappa^{-1}(\kappa) = \hat{\kappa}_{\mathrm{S}};\ \kappa \in \mathcal{T}_h\}. \end{aligned}$$

Given that $\mathbf{v} \in \left[H^1(\kappa)\right]^m$ for each $\kappa \in \mathcal{T}_h$, we denote by $\mathbf{v}^+$ (respectively, $\mathbf{v}^-$) the interior (respectively, exterior) trace of $\mathbf{v}$ on $\partial\kappa$.

The hp–DGFEM approximation of (19) is defined as follows: find $\mathbf{u}_{\mathrm{DG}}$ in $S^{\mathbf{p}}(\Omega,\mathcal{T}_h,\mathbf{F})$ such that

$$\begin{aligned} \mathcal{N}(\mathbf{u}_{\mathrm{DG}},\mathbf{v}) \equiv \sum_{\kappa\in\mathcal{T}_h} \Bigg\{ -\int_\kappa \mathcal{F}(\mathbf{u}_{\mathrm{DG}}) \cdot \nabla\mathbf{v}\,\mathrm{d}x + \int_{\partial\kappa} \mathcal{H}(\mathbf{u}_{\mathrm{DG}}^+, \mathbf{u}_{\mathrm{DG}}^-, \mathbf{n}_\kappa)\,\mathbf{v}^+\,\mathrm{d}\sigma \\ + \int_\kappa \varepsilon \nabla\mathbf{u}_{\mathrm{DG}} \cdot \nabla\mathbf{v}\,\mathrm{d}x \Bigg\} = 0 \end{aligned} \tag{20}$$

for all $\mathbf{v} \in S^{\mathbf{p}}(\Omega,\mathcal{T}_h,\mathbf{F})$; cf. [12,15], for example. Here, $\mathcal{H}(\cdot,\cdot,\cdot)$ denotes a *numerical flux* function, assumed to be Lipschitz continuous, consistent and conservative. We note that the choice of the numerical flux function is completely independent of the finite element space employed; in Section 3.3 we employ the (local) Lax–Friedrichs flux function. In (20), ε denotes the coefficient of artificial viscosity defined by

$$\varepsilon|_\kappa = C_\varepsilon \left(\frac{h_\kappa}{p_\kappa}\right)^{2-\beta} |\,\mathrm{div}\mathcal{F}(\mathbf{u}_{\mathrm{DG}}|_\kappa)|\,,$$

where C_ε is a positive constant and $0 < \beta < 1/2$; cf. Jaffre *et al.* [15]. Here, for elements $\kappa \in \mathcal{T}_h$ whose boundary intersects that of the computational domain Ω, we replace $\mathbf{u}_h^-$ by appropriate boundary/initial conditions on the portion of $\partial\kappa$ for which $\partial\kappa \cap \partial\Omega \neq \emptyset$.

3.2 A posteriori error analysis

In this section, we present a brief overview of duality–based Type I *a posteriori* error estimation for controlling the error in the approximation of a given output or target functional $J(\cdot)$ of the solution. For a complete account we refer to the series of papers [12,14,24,25]; see also [13,20,22] for related work.

Before we embark on our *a posteriori* error analysis, we shall introduce some notation. We write $\mathcal{M}(\mathbf{u}, \mathbf{u}_{\mathrm{DG}}; \cdot, \cdot)$ to denote the mean–value linearisation of $\mathcal{N}(\cdot, \cdot)$ defined by

$$\begin{aligned}\mathcal{M}(\mathbf{u}, \mathbf{u}_{\mathrm{DG}}; \mathbf{u} - \mathbf{u}_{\mathrm{DG}}, \mathbf{v}) &= \mathcal{N}(\mathbf{u}, \mathbf{v}) - \mathcal{N}(\mathbf{u}_{\mathrm{DG}}, \mathbf{v}) \\ &= \int_0^1 \mathcal{N}'_{\mathbf{u}}[\theta\mathbf{u} + (1-\theta)\mathbf{u}_{\mathrm{DG}}](\mathbf{u} - \mathbf{u}_{\mathrm{DG}}, \mathbf{v}) \, \mathrm{d}\theta \qquad (21)\end{aligned}$$

for all $\mathbf{v}$ in V, where V is a suitable function space such that $S^{\mathbf{p}}(\Omega, \mathcal{T}_h, \mathbf{F}) \subset V$. Here, $\mathcal{N}'_{\mathbf{u}}[\mathbf{w}](\cdot, \mathbf{v})$ denotes the Gateaux derivative of $\mathbf{u} \mapsto \mathcal{N}(\mathbf{u}, \mathbf{v})$, for $\mathbf{v} \in V$ fixed, at some $\mathbf{w}$ in V. The linearisation defined in (21) is only a *formal* calculation, in the sense that $\mathcal{N}'_{\mathbf{u}}[\mathbf{w}](\cdot, \cdot)$ may not in general exist. Instead, a suitable approximation to $\mathcal{N}'_{\mathbf{u}}[\mathbf{w}](\cdot, \cdot)$ must be determined, for example, by computing appropriate finite difference quotients of $\mathcal{N}(\cdot, \cdot)$, cf. [12]. For the proceeding analysis, we *assume* that the linearisation (21) is well–defined. Under this hypothesis, we introduce the following *dual* problem: find $\mathbf{z} \in V$ such that

$$\mathcal{M}(\mathbf{u}, \mathbf{u}_{\mathrm{DG}}; \mathbf{w}, \mathbf{z}) = J(\mathbf{w}) \quad \forall \mathbf{w} \in V. \qquad (22)$$

We assume that (22) possesses a unique solution; of course, the validity of this assumption depends on both the definition of $\mathcal{M}(\mathbf{u}, \mathbf{u}_{\mathrm{DG}}; \cdot, \cdot)$ and the choice of the linear functional under consideration, cf. [12]. For the proceeding error analysis, we must therefore *assume* that the dual problem (22) is well–posed. We then have the following result.

Theorem 1. *Let* $\mathbf{u}$ *and* $\mathbf{u}_{\mathrm{DG}}$ *denote the solutions to (19) and (20), respectively, and suppose that the dual problem (22) is well–posed. Then,*

$$J(\mathbf{u}) - J(\mathbf{u}_{\mathrm{DG}}) = \mathcal{E}_\Omega \equiv \sum_{\kappa \in \mathcal{T}_h} \eta_\kappa, \qquad (23)$$

where

$$\begin{aligned}\eta_\kappa = \int_\kappa \mathbf{r}_{h,p} \cdot (\mathbf{z} - \mathbf{z}_{h,p}) \, \mathrm{d}x &+ \int_{\partial\kappa} \boldsymbol{\rho}_{h,p} \cdot (\mathbf{z} - \mathbf{z}_{h,p})^+ \, \mathrm{d}\sigma \\ &- \int_\kappa \varepsilon \nabla \mathbf{u}_{\mathrm{DG}} \cdot \nabla(\mathbf{z} - \mathbf{z}_{h,p}) \, \mathrm{d}x \qquad (24)\end{aligned}$$

for all $\mathbf{z}_{h,p}$ *in* $S^{\mathbf{p}}(\Omega, \mathcal{T}_h, \mathbf{F})$. *Here,*

$$\mathbf{r}_{h,p}|_\kappa = -\mathrm{div}\mathcal{F}(\mathbf{u}_{\mathrm{DG}}) \quad \textit{and} \quad \boldsymbol{\rho}_{h,p}|_\kappa = \mathcal{F}(\mathbf{u}_{\mathrm{DG}}) \cdot \mathbf{n}_\kappa - \mathcal{H}(\mathbf{u}_{\mathrm{DG}}^+, \mathbf{u}_{\mathrm{DG}}^-, \mathbf{n}_\kappa)$$

denote the internal and boundary finite element residuals, respectively, defined on each $\kappa \in \mathcal{T}_h$.

Proof. The proof follows by recalling the linearity of $J(\cdot)$, and exploiting the Galerkin orthogonality property of the hp–DGFEM (20); see [12], for details.

Based on the general error representation formula derived in Theorem 1, *a posteriori* error estimates bounding the error in the computed functional $J(\cdot)$ may be deduced. We shall confine ourselves to considering a Type I *a posteriori* error bound; it is a straightforward consequence of the error representation formula stated in the previous theorem.

Corollary 1. *Under the assumptions of Theorem 1, we have*

$$|J(\mathbf{u}) - J(\mathbf{u}_{\mathrm{DG}})| \leq \mathcal{E}_{|\Omega|} \equiv \sum_{\kappa \in \mathcal{T}_h} |\eta_\kappa| \,. \tag{25}$$

Proof. The error bound (25) follows from (23) by application of the triangle inequality.

We note that for nonlinear hyperbolic conservation laws, both the error representation formula (23) and the Type I *a posteriori* error bound (25) depend on the unknown analytical solutions to the primal and dual problems. Thus, in order to render these quantities computable, both $\mathbf{u}$ and $\mathbf{z}$ must be replaced by suitable approximations. To this end, the linearisation leading to $\mathcal{M}(\mathbf{u}, \mathbf{u}_{\mathrm{DG}}; \cdot, \cdot)$ is performed about $\mathbf{u}_{\mathrm{DG}}$ and the dual solution $\mathbf{z}$ is replaced by a discontinuous Galerkin approximation $\hat{\mathbf{z}}_{\mathrm{DG}}$ computed on the same mesh $\mathcal{T}_h$ as for the primal solution $\mathbf{u}_{\mathrm{DG}}$, but with a higher degree polynomial, i.e., $\hat{\mathbf{z}}_{\mathrm{DG}} \in S^{\hat{\mathbf{p}}}(\Omega, \mathcal{T}_h, \mathbf{F})$, $\hat{\mathbf{p}} = \mathbf{p} + \mathbf{p}_{\mathrm{INC}}$; in Section 3.3, we set $\mathbf{p}_{\mathrm{INC}} = \mathbf{1}$.

For the design of an appropriate hp–adaptive algorithm, we employ the refinement indicator $|\hat{\eta}_\kappa|$ to first mark the elements for refinement or derefinement using the fixed fraction mesh refinement strategy; see [23], for example. Here, $\hat{\eta}_\kappa$ is defined analogously to η_κ, cf. equation (24), with $\mathbf{z}$ replaced by $\hat{\mathbf{z}}_{\mathrm{DG}}$. Once an element $\kappa \in \mathcal{T}_h$ has been flagged for refinement or derefinement, a decision must be made whether the local mesh size h_κ or the local degree p_κ of the approximating polynomial should be adjusted accordingly. The choice to perform either h–refinement/derefinement or p–refinement/derefinement is dependent on the local smoothness of the primal and dual solutions $\mathbf{u}$ and $\mathbf{z}$, respectively, cf. [14,25]. More precisely, for each element κ in the computational mesh $\mathcal{T}_h$, we estimate the local Sobolev regularities k_κ and l_κ of the primal and dual solutions, respectively, using the Root Test algorithm, cf. Section 2. Then, if the element κ has been marked for refinement, a p–enrichment will be performed if either k_κ or l_κ is larger than $p_\kappa + 1$; otherwise

κ is subdivided. On the other hand, if the element κ has been flagged for derefinement, then κ is coarsened if either k_κ or l_κ is larger than $p_\kappa + 1$; otherwise the degree p_κ is reduced by one, cf. [14].

We remark that the natural set of basis functions employed for the *hp*–DGFEM on quadrilateral elements consists of tensor product Legendre polynomials. Thereby, the regularity estimation algorithms developed in Section 2 can be applied directly to $\mathbf{u}_{\mathrm{DG}}$ and $\mathbf{z}_{\mathrm{DG}}$ in order to estimate the local smoothness of the functions $\mathbf{u}$ and $\mathbf{z}$, respectively. If a different polynomial basis is employed for either $\mathbf{u}_{\mathrm{DG}}$ or $\mathbf{z}_{\mathrm{DG}}$, then it is a simple task to first rewrite these local expansions in terms of a Legendre basis in order to estimate their local Sobolev regularity. As a final note, we point out that here we do not modify the predicted regularity in order to account for boundary singularities; however, this will be important for the numerical approximation of elliptic partial differential equations.

3.3 Numerical Experiment

In this section we present a numerical example to demonstrate the practical performance of the proposed *hp*–adaptive finite element algorithm based on estimating the local regularities of the primal and dual solutions $\mathbf{u}$ and $\mathbf{z}$, respectively, using the Root Test algorithm. Here, the we set the refinement and coarsening fractions to be 20% and 10%, respectively.

Burgers' problem Let is consider the unsteady inviscid Burgers' equation $u_t + \left((1/2)\,u^2\right)_x$ for the scalar variable $\mathbf{u} \equiv u$; on writing $x_1 = x$ and $x_2 = t$, we have $u_{x_2} + \left((1/2)\,u^2\right)_{x_1} = 0$, on the (space–time) domain $\Omega = (0,3)\times(0,2)$, subject to the initial condition

$$u(x,0) = \begin{cases} 2\,\sin^2(\pi x)\,, & 0 \le x \le 1\,, \\ \sin^2(\pi x)\,, & 1 \le x \le 2\,, \\ 0\,, & 2 \le x \le 3\,, \end{cases}$$

and boundary condition $u(0,x_2) = 0$, for $x_2 \in [0,2]$. The analytical solution to this problem consists of two smooth 'hills' which form shock waves as time increases. These shocks will eventually merge to form a single line of discontinuity in the (x_1,x_2)–plane. Here, we select the functional of interest $J(\cdot)$ to be the value of the solution before these two shocks interact with one another. More precisely, we choose $J(u) = u(2.4, 1.6)$; thereby, the true value of the functional is $J(u) = 0.681745280066953785$.

In Fig. 9 we show the regions in the computational domain which are classified as being smooth and nonsmooth for both the primal and dual solutions after 2 and 11 adaptive mesh refinements. Recalling that k_κ and l_κ denote the (predicted) regularities of the primal and dual solutions u and z, respectively, for each element κ in the mesh $\mathcal{T}_h$, in Figs. 9(a) & (c), resp. Figs. 9(b) & (d), we shade the element white if $k_\kappa > p_\kappa + 1$, resp. $l_\kappa > p_\kappa + 1$, or grey

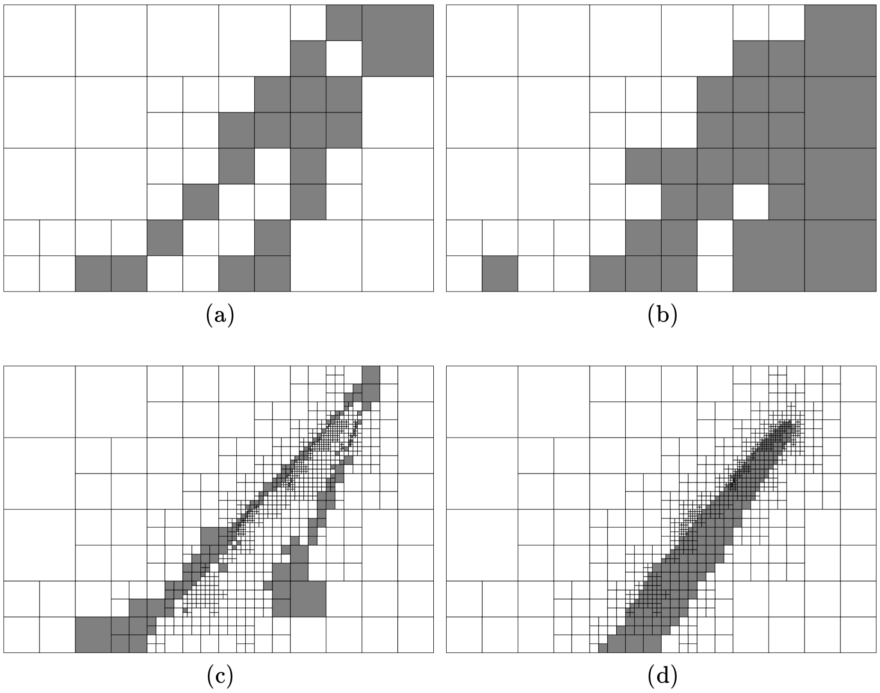

Fig. 9. Burgers' equation. Elements marked as nonsmooth (grey) or smooth (white) for: (a) & (b) Primal and dual solution, respectively, after 2 adaptive refinements; (c) & (d) Primal and dual solution, respectively, after 11 adaptive refinements

otherwise; thereby, grey shaded elements indicate regions where the solution is locally non-smooth. From Fig. 9(a), we see that even on this coarse mesh, the regions of the computational domain where the shocks in u are located are broadly identified; these regions are clearly resolved on the finer mesh shown in Fig. 9(c).

We note that the dual solution z consists of a 'spike' which is transported upstream along the single characteristic passing through the point of interest. In Fig. 9(b) we see that the region where this spike is located is again broadly identified, though the mesh here is too coarse to determine where the point of interest is located in relation to the shocks present in u. However, as the mesh is adaptively refined, we clearly see that the grey region has focused in on the characteristic curve along which the dual solution z is nonsmooth, cf. Fig. 9(d).

In Fig. 10 we show the hp–mesh after 11 adaptive mesh refinements. For clarity, we show the h–mesh alone, as well as the corresponding distribution of the polynomial degree and the percentage of elements with that degree. Here,

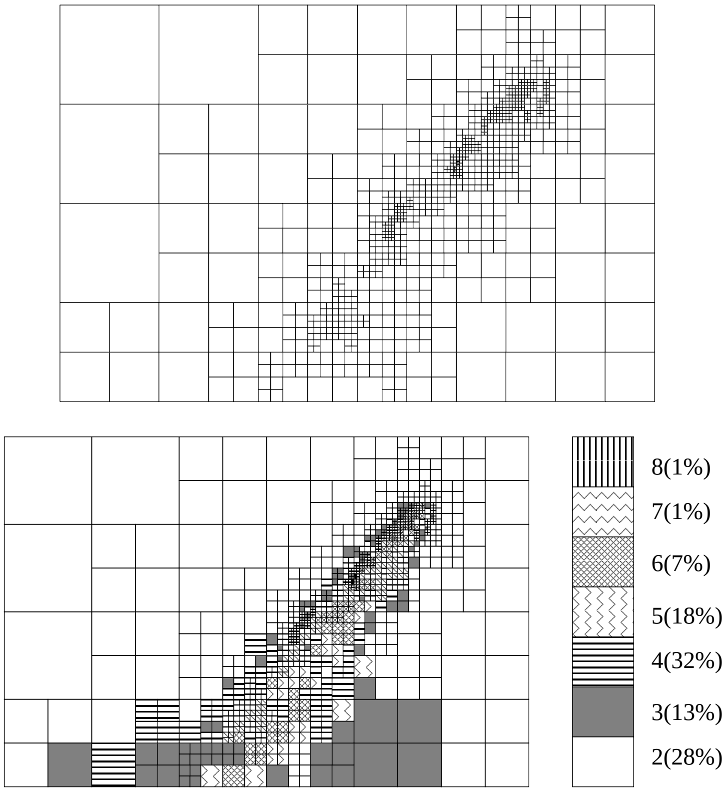

Fig. 10. Burgers' equation. h– and hp–meshes after 11 refinements, with 1002 elements and 23288 degrees of freedom; here, $|J(u) - J(u_{\rm DG})| = 3.587 \times 10^{-8}$

we see that the h–mesh has been refined in the region upstream of the point of interest, thereby isolating the smooth region of u from the two interacting shock waves; this renders the subsequent p–refinement in this region much more effective.

Finally, in Fig. 11(a) we plot $|J(u) - J(u_{\rm DG})|$, using both h– and hp–refinement against the square–root of the number of degrees of freedom on a linear–log scale. Here, we see that after the initial transient, the error in the computed functional using hp–refinement becomes (on average) a straight line, thereby indicating exponential convergence of $J(u_{\rm DG})$ to $J(u)$, despite the fact that u is only piecewise continuous; this occurs since u is a real analytic function in the region of the computational domain that influences the value of the target functional of interest. Fig. 11(a) also demonstrates the superiority of the adaptive hp–refinement strategy over a traditional adaptive h–refinement algorithm. Indeed, on the final mesh the true error between

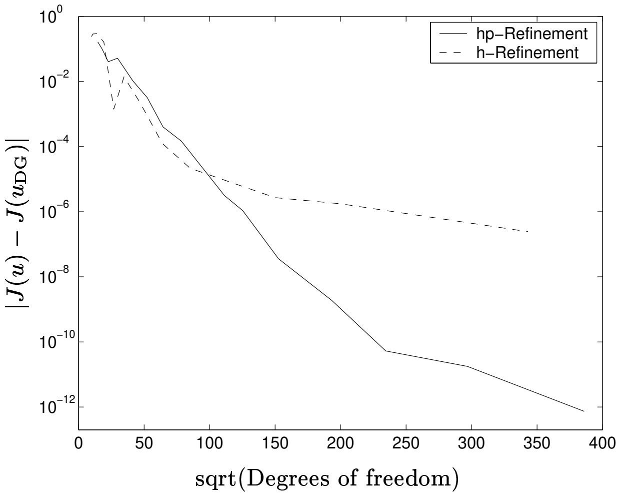

(a)

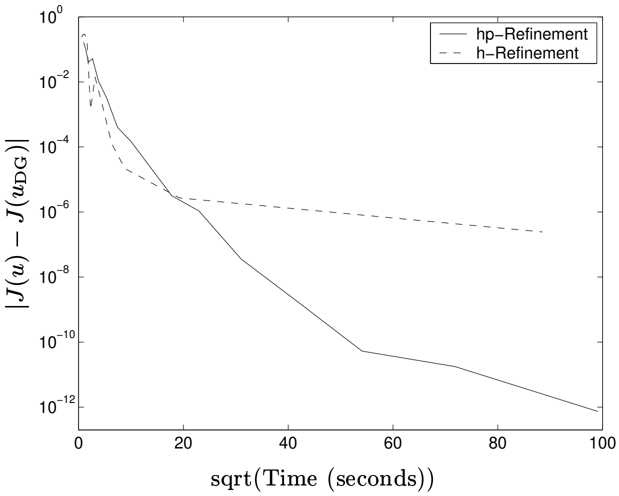

(b)

Fig. 11. Burgers' equation. Comparison between h– and hp–adaptive mesh refinement: (a) $|J(u) - J(u_{\mathrm{DG}})|$ versus number of degrees of freedom; (b) $|J(u) - J(u_{\mathrm{DG}})|$ versus computational time

$J(u)$ and $J(u_{\mathrm{DG}})$ using hp–refinement is over 5 orders of magnitude smaller than the corresponding quantity when h–refinement is employed alone. Furthermore, from Fig. 11(b) we observe that the hp–refinement algorithm also outperforms the h–refinement strategy, when comparing the error in the com-

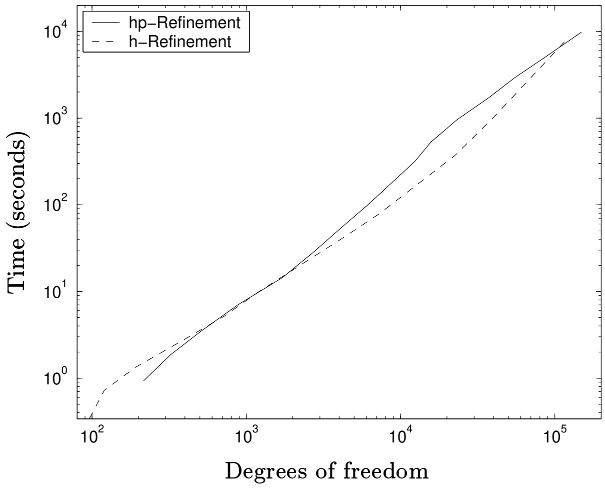

Fig. 12. Burgers' equation. Computational time versus number of degrees of freedom

puted target functional with respect to the computational cost. Indeed, Fig. 12 indicates that for the *hp*–DGFEM, the cost per degree of freedom when *hp*–refinement is employed is comparable to that of using *h*–refinement.

4 Concluding remarks

In this paper we have developed an automatic algorithm for estimating the local Sobolev regularity of a given square-integrable function by monitoring the decay rate of its Legendre expansion coefficients. This approach is computationally very cheap; moreover, it is capable of estimating the local smoothness properties of a function in each coordinate direction separately which will be important in the design of anisotropic *hp*–mesh refinement strategies.

On the basis of this algorithm, we have designed and implemented an *hp*–adaptive discontinuous Galerkin finite element method for the solution of nonlinear systems of hyperbolic conservation laws. The superiority of this general *hp*–adaptive strategy over a traditional *h*–refinement algorithm where the degree p of the approximating polynomial is kept fixed at some low value has been demonstrated numerically.

References

1. S. Adjerid, M. Aiffa, J.E. Flaherty, *Computational methods for singularly perturbed systems.* In J. Cronin and R.E. O'Malley, editors, Singular Perturbation Concepts of Differential Equations, AMS, Providence, 1998.

2. M. Ainsworth and J.T. Oden, *A Posteriori Error Estimation in Finite Element Analysis.* Series in Computational and Applied Mathematics. Elsevier, 1996.
3. M. Ainsworth and B. Senior, *An adaptive refinement strategy for hp–finite element computations.* Appl. Numer. Math. 26:165–178, 1998.
4. I. Babuška and M. Suri, *The hp-Version of the Finite Element Method with quasiuniform meshes.* M^2AN Modél. Math. Anal. Numér. 21:199–238, 1987.
5. R. Becker and R. Rannacher, *An optimal control approach to a-posteriori error estimation in finite element methods.* In A. Iserles, editor, Acta Numerica, 2001.
6. C. Bernardi, N. Fiétier and R. G. Owens, *An error indicator for mortar element solutions to the Stokes problem.* IMA J. Num. Anal. 21:857–886, 2001.
7. K.S. Bey, A. Patra and J.T. Oden, *hp–version discontinuous Galerkin methods for hyperbolic conservation laws: a parallel adaptive strategy.* Internat. J. Numer. Methods Engrg. 38:3889–3908, 1995.
8. L. Demkowicz, W. Rachowicz and Ph. Devloo, *A Fully Automatic hp–Adaptivity.* J. Sci. Comp. (to appear).
9. S.A. Douglass, *Introduction to Mathematical Analysis.* Addison Wesley, 1996.
10. K. Eriksson, D. Estep, P. Hansbo and C. Johnson, *Introduction to adaptive methods for differential equations.* In A. Iserles, editor, Acta Numerica, pp. 105–158, 1995.
11. W. Gui and I. Babuška, *The h, p and h–p versions of the finite element method in 1 Dimension. Part III. The adaptive h–p version.* Numer. Math. 49:659–683, 1986.
12. R. Hartmann and P. Houston, *Adaptive Discontinuous Galerkin Finite Element Methods for Nonlinear Hyperbolic Conservation Laws.* Leicester University Technical Report 2001/20, 2001. (Submitted).
13. P. Houston, R. Rannacher and E. Süli, *A posteriori error analysis for stabilised finite element approximations of transport problems.* Comput. Meth. Appl. Mech. Engrg. 190(11-12):1483–1508, 2000.
14. P. Houston and E. Süli, *hp–Adaptive discontinuous Galerkin finite element methods for hyperbolic problems.* SIAM J. Sci. Comp. 23(4):1225-1251, 2001.
15. J. Jaffre, C. Johnson and A. Szepessy, *Convergence of the discontinuous Galerkin finite element method for hyperbolic conservation laws.* Math. Models Methods Appl. Sci. 5(3):367–386, 1995.
16. C. Mavriplis, *Adaptive mesh strategies for the spectral element method.* Comput. Methods. Appl. Mech. Engrg. 116:77–86, 1994.
17. J.T. Oden and A. Patra, *A parallel adaptive strategy for hp finite elements.* Comput. Methods. Appl. Mech. Engrg. 121:449–470 1995.
18. J.T. Oden, A. Patra and Y.S. Feng, *An hp adaptive strategy.* In A.K. Noor, editor, Adaptive, Multilevel, and Hierarchical Computational Strategies, AMD-157, ASME, New York, pages 23–26, 1992.
19. W. Rachowicz, L. Demkowicz and J.T. Oden, *Toward a universal h–p adaptive finite element strategy, Part 3. Design of h–p meshes.* Comput. Methods. Appl. Mech. Engrg. 77:181–212, 1989.
20. R. Rannacher, *Adaptive finite element methods*, in H. Bulgak and C. Zenger, eds., Proc. NATO-Summer School *Error Control and Adaptivity in Scientific Computing*, Kluwer, Academic Publishers, 247–278, 1998.
21. Ch. Schwab, *p– and hp–Finite Element Methods. Theory and Applications to Solid and Fluid Mechanics.* Oxford University Press, Oxford, 1998.

22. E. Süli, *A posteriori error analysis and adaptivity for finite element approximations of hyperbolic problems.* In: D. Kröner, M. Ohlberger and C. Rohde (Eds.) An Introduction to Recent Developments in Theory and Numerics for Conservation Laws. Lecture Notes in Computational Science and Engineering. Vol. 5, pages 123–194. Springer-Verlag, 1998.
23. E. Süli and P. Houston, *Adaptive finite element approximation of hyperbolic problems.* von Karman Institute Lecture Series Monographs (to appear).
24. E. Süli, P. Houston and Ch. Schwab, *hp–Finite element methods for hyperbolic problems.* In: J.R. Whiteman, editor, The Mathematics of Finite Elements and Applications X. MAFELAP 1999. Elsevier, 143–162, 2000.
25. E. Süli, P. Houston and B. Senior, *hp–Discontinuous Galerkin finite element methods for nonlinear hyperbolic problems.* Int. J. Numer. Meth. Fluids (to appear).
26. B. Szabó and I. Babuška, *Finite Element Analysis.* J. Wiley & Sons, New York, 1991.
27. J. Valenciano and R.G. Owens, *An h–p adaptive spectral element method for Stokes flow.* Appl. Numer. Math. 33:365–371, 2000.
28. R. Verfürth, *A Review of a Posteriori Error Estimation and Adaptive Mesh-Refinement Techniques.* B.G. Teubner, Stuttgart, 1996.